



## Spectroscopic anatomy of a meteor trail cross section with the European Southern Observatory Very Large Telescope

Peter JENNISKENS,<sup>1\*</sup> Emmanuel JEHIN,<sup>2</sup> Remi A. CABANAC,<sup>3</sup> Christophe O. LAUX,<sup>4</sup> and Iain D. BOYD<sup>5</sup>

<sup>1</sup>SETI Institute, 2035 Landings Drive, Mountain View, California 94043, USA

<sup>2</sup>European Southern Observatory, Alonso de Cordova 3107, Casilla 19001, Santiago 19, Chile

<sup>3</sup>Departamento de Astronomia y Astrofisica Pontificia Universidad Catolica de Chile, Campus San Joaquin, Casilla 206 Santiago 22, Chile

<sup>4</sup>Ecole Centrale Paris, Laboratoire EM2C, Grande Voie des Vignes, 92290 Chatenay-Malabry, France

<sup>5</sup>Department of Aerospace Engineering, University of Michigan, 3012 Francois-Xavier Bagnoud Building, 1320 Beal Avenue, Ann Arbor, Michigan 48109–2140, USA

\*Corresponding author. E-mail: [pjenniskens@mail.arc.nasa.gov](mailto:pjenniskens@mail.arc.nasa.gov)

(Received 9 June 2003; revision accepted 2 March 2004)

---

**Abstract**—A meteor spectrum was recorded serendipitously at the European Southern Observatory (ESO) Very Large Telescope (VLT) during a long exposure in long-slit spectroscopic mode with FORS1. The  $-8$  magnitude fireball crossed the narrow  $1'' \times 7'$  slit during the observation of a high  $z$  supernova in normal service mode operation on May 12, 2002. The spectrum covered the range of 637–1050 nm, where the meteor's air plasma emissions from  $N_2$ , N, and O dominate. Carbon atom emission was not detected in the relatively unexplored wavelength range above 900 nm, but the observed upper limit was only 3 sigma less than expected from the dissociation of atmospheric  $CO_2$ . The meteor trail was resolved along the slit, and the emission had a Gaussian distribution with a dimension of  $FWHM = 7.0 (\pm 0.4) * \sin(\alpha) * H$  (km)/90 m, where  $\alpha$  is the unknown angle between the orientation of the meteor path and slit and  $H$  the assumed altitude of the meteor in km. To our knowledge, this is the first observation of a spatially resolved spectrum across a meteor trail. Unlike model predictions, the plasma excitation temperature varied only from about 4,300 to 4,365 K across the trail, based on the ratio of atomic and molecular nitrogen emissions. Unfortunately, we conclude that this was because the meteor at 100 km altitude was out of focus.

---

### INTRODUCTION

Meteor spectra (Bronshten 1983) have on occasion been obtained serendipitously during photographic star spectra surveys with Schmidt cameras equipped with objective-mounted gratings and prisms (Millman 1949, 1980). To capture a meteor spectrum with the now-common high-dispersion slit-spectrographs at astronomical observatories is difficult because of the small effective field of view of a slit. Moreover, a rare relatively bright meteor is required to register in the brief moment that the meteor crosses the narrow slit. With increasing numbers of large telescopes in the world, however, it may come as no surprise that such a bright meteor crossed the long  $1'' \times 7'$  slit of the FORS1 spectrograph at the European Southern Observatory (ESO) Very Large Telescope (VLT) on May 12, 2002.

This is the first such serendipitous record of a meteor spectrum to our knowledge. Earlier, Borovička and Zamorano (1995) reported on the detection of scattered light from a

bright fireball that just missed the slit of the 2.2-m telescope at the Calar Alto Observatory. Six lines were detected in the 660–715 nm range, the most remarkable being a possible detection of the lithium line at 670.8 nm.

Unlike these earlier observations, the new data set provides a spatially resolved spectroscopic anatomy across the meteor trail, covering the wavelength range of 637–1050 nm. This range is dominated by emissions from air atoms and molecules in the meteor path and teach us about the collision processes in the wake of a meteoroid. With the advance of cooled CCD cameras, these air plasma emissions have only recently been studied in detail up to about 880 nm (Jenniskens et al. 2000, 2004a). Earlier photographic studies were typically sensitive only up to about 600 nm and traditionally focussed on the metal atom ablation lines at visible wavelengths (Ceplecha 1973; Harvey 1973; Borovička 1993; Borovička et al. 1999). The range above 880 nm remains relatively unexplored and contains unique lines of atomic carbon.

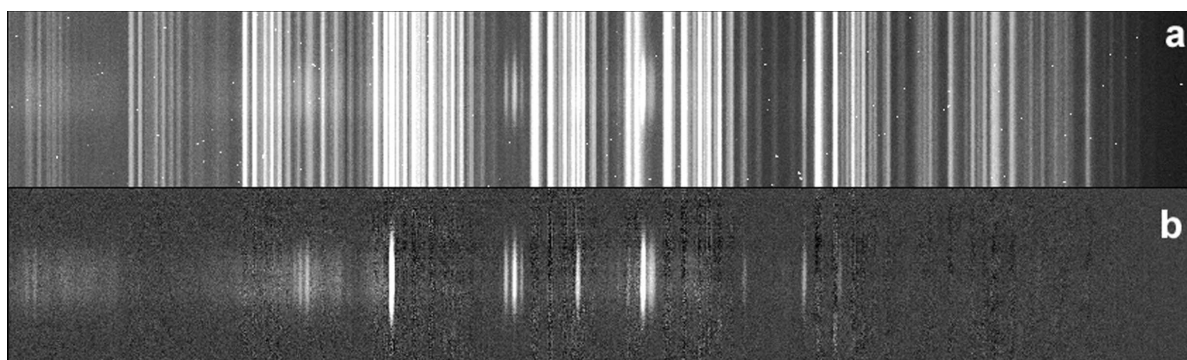


Fig. 1. Raw CCD part frame of the ESO VLT meteor of May 12, 2002: a) meteor + sky; b) meteor after sky subtraction.

The width of the trail is determined by the radial displacement of air molecules (and their collision products) after hitting the meteoroid and its ablation vapor cloud, during the collisional cascade that follows the initial collision. This is a function of the speed of the meteoroid and the mean-free path of the molecules at altitude, which is proportional to the inverse of the ambient air density ( $l \sim n_a^{-1}$ ). Radar observations, however, show a weaker atmospheric density dependence, meaning  $l \sim n_a^{-s}$  with  $0 < s < 1$  (Baggaley 1970, 1980, 1981).

The theory of radar echo from an under-dense meteor train is based on the assumption of a Gaussian initial distribution of ions in the train (McKinley 1961; Jones 1995). The distribution of light intensity across the slit in our new data can be used to test this hypothesis. Earlier direct measurements of the width of meteor trails (of order 1–6 m) were based on photographic observations, where the spatial resolution typically is not high enough to study the distribution of light across the trail (Cook et al. 1959, 1962, and references therein).

## THE OBSERVATION

During a 20-min exposure in long-slit spectroscopic mode with the instrument FORS1 (in service mode) at the ESO Very Large Telescope ( $-24^{\circ}62'51''\text{S}$ ,  $-70^{\circ}40'27''\text{W}$ ) an unusual signal was detected in an exposure starting at 03:01:11.428 UT May 12, 2002, when the solar longitude was  $\lambda_o = 51.201$  (Eq. J2000). The unusual signal was only seen on the FORS1 spectrum, and unfortunately, there is no information regarding the orientation of the meteor path. There was no all-sky image taken at that time, nobody reported a visual observation, and there was nothing seen on the acquisition image.

The full data set consisted of three consecutive exposures (1200 s) of the same field at right ascension = 14h01m39.5s and declination =  $+04^{\circ}37'03.0''$  (J2000), and only one of the three exposures showed the peculiar signal. At the start of the exposure, the telescope was pointed at an elevation of  $60.2^{\circ}$  (azimuth  $11.8^{\circ}$  from north) at a mean air mass of 1.15. The seeing was full-width-at-half-maximum (FWHM) =  $1.4''$ ,

measured from a star on the slit. The spectrograph was set up to have a slit  $416.75''$  long and only  $1''$  wide, with a position angle of  $178.69^{\circ}$  at the start of exposure ( $N = 0^{\circ}$ ,  $E = 90^{\circ}$ ). The choice of prism 3001 and order filter OG590+72 resulted in a dispersion of  $108 \text{ \AA}/\text{mm}$  or  $0.259 \text{ nm}/\text{pixel}$  or a spectral resolution  $\lambda/\Delta\lambda = 660$  at the central wavelength of  $860 \text{ nm}$ .

The exposure containing the anomalous signal is shown in Fig. 1, both before and after subtraction of the sky background. The CCD size measures  $2048 \times 2048$  pixels. The spatial extension of the spectrum is about 150 pixels or  $30''$  (pixel scale =  $0.200''/\text{pix.}$ ). The meteor was centered at about pixel 329, and the extraction of the signal was done from line 260 to 410.

The following procedure was used to reduce the data with the IRAF (NOAO) analysis program. After subtraction of the CCD bias, the image was divided by a normalized flat field to correct for vignetting and pixel-to-pixel sensitivity variations. A 2D-wavelength calibration was made, using a Th-Ar-He lamp, to remove the curvature of the lines. The sky background was subtracted by fitting a second order Chebychev polynomial to two windows located just above and below the meteor spectrum. Because of the long exposure time, the airglow sky lines were quite intense and could not be removed completely.

A 1D spectrum was extracted (Fig. 2) with the rejection of cosmic rays. The result was flux-calibrated using the response to spectrophotometric standard star Irt3218. The reduction of the spectrophotometric standard star was done with the same reduction steps. The extinction for the altitude of Paranal (using the IRAF standard extinction curve) and airmass were taken into account in the flux calibration, but the spectrum was not corrected for absorption by water vapor. Water vapor absorption was negligibly small in this wavelength range.

## IDENTIFICATION AS A METEOR SPECTRUM

### The Identification of Lines and Bands

The unusual emission (Fig. 2) is identified as originating from a meteor. Above  $600 \text{ nm}$ , meteor emission is usually

Table 1. Identified emission lines and bands.

Wavelength (nm)		Identification	$\Sigma$ intensity (au)		Notes
Measured	Theory <sup>a</sup>		Measured		
640–690	640–690	N <sub>2</sub> 1+; $\Delta v = +3$	674		
645.54	645.776	O I	22		
648.44	648.449	N I	23		blend 648.45/648.66
705–766	705–766	N <sub>2</sub> 1+; $\Delta v = +2$	773		
742.49	742.569	N I	6		
744.37	744.435	N I	15		
746.83	747.037	N I	30		
777.36	777.408	O I	361		blend 777.41/777.63/777.75
791.62	791.760	N I	11		blend 790.15/791.76
815–893	815–893	N <sub>2</sub> 1+; $\Delta v = +1$	268		
818.65	818.711	N I	41		blend 818.71/819.03
821.74	821.860	N I	87		blend 820.26/821.30/821.86/822.54
824.27	824.466	N I	24		
844.64	844.868	O I	80		blend 844.86/844.87/844.91
856.85	857.009	N I	3		
859.52	859.636	N I	6		
862.95	863.161	N I	14		
865.94	865.826	N I	8		
868.20	868.267	N I	241		blend 868.27/868.58/868.85
871.15	871.410	N I	74		870.56/871.41/872.12/873.13/874.97
--	880.917	Mg I	<2		not seen
904.79	904.836	N I	18		blend 904.84/905.20/905.24 906.30
--	909.733	C I	<2		906.39/906.50/908.08/909.10/909.73
919.90	921.053	N I	5		919.00/919.04/919.21/921.01/921.05
926.37	926.339	O I	49		blend 926.34/926.53/926.86
939.23	938.938	N I	21		blend 938.94/939.54
--	940.831	C I	<5		not seen
--	960.567	C I	<3		not seen
--	966.108	C I	<2		not seen
1011.20	1011.166	N I	6		1010.79/1011.17/1011.53/1011.74

<sup>a</sup>If blended lines, strongest feature is given.

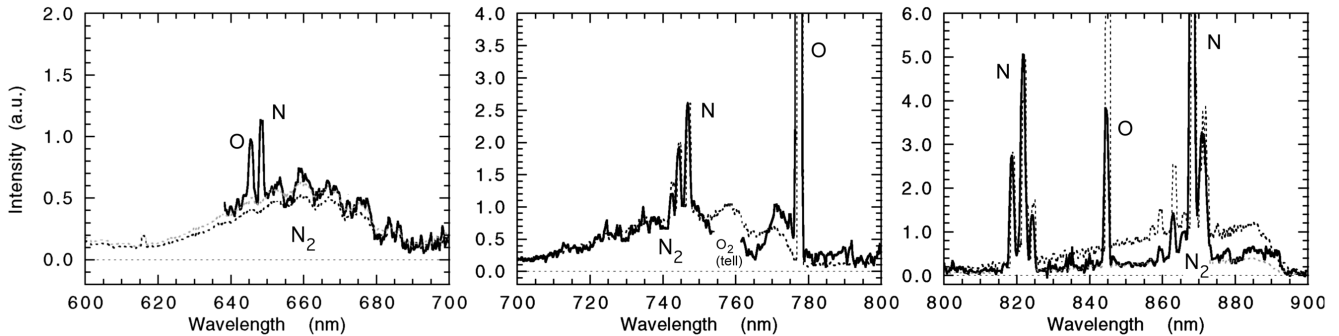


Fig. 2. Details of the May 12, 2002 meteor spectrum (solid line). Flux is in units of  $10^{-16}$  W/cm<sup>2</sup>/Å if a continuum source was exposed for 1200 s. The dashed line is a NEQAIR2 model LTE air plasma spectrum, relevant for 95 km altitude ( $P = 10^{-6}$  atm) and  $T = 4,340$  K. Note that the model under-predicts the intensity of the  $\Delta v = +3$  band series of N<sub>2</sub> (left), while overpredicting the  $\Delta v = +1$  band series (right). Thin dashed lines show the model of each individual band scaled to the observed band strength (in arbitrary units).

dominated by air plasma emissions from N<sub>2</sub>, N, and O. Indeed, the spectrum is very similar to, for example, one of our  $-2$  magnitude Perseids that was captured with a cooled CCD camera at the Fremont Peak Observatory (California) on August 13, 2002 (Fig. 3). Atomic lines of N, O, and the first

positive  $B^3\Pi_g \rightarrow A^3\Pi_u^+$  bands of N<sub>2</sub> are present, which have relatively high upper state energies of 7–12 eV.

There are few metal atom ablation lines in this part of the spectrum. The 880-nm line of meteoric Mg I that is clearly recognized in the Perseid (Fig. 3) was not present in the ESO

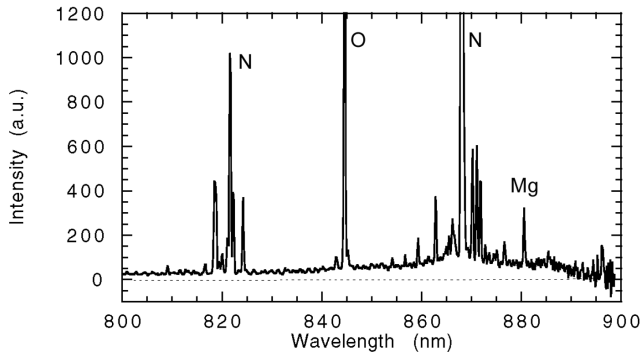


Fig. 3. Perseid meteor spectrum obtained with a slit-less CCD spectrograph on August 13, 2002 at 10:24:33 UT. Note the presence of the meteoric metal Mg I emission line not seen in the ESO VLT spectrum.

VLT meteor. There was also no clear sign of the sometimes strong K I doublet at 766.7 and 770.1 nm. We checked for other possible neutral and single ionized metal atom line emissions, but none were found. Indeed, all new atomic lines in the ESO VLT meteor were identified as either oxygen or nitrogen atomic emissions.

The emission features identified above 3 sigma are listed in Table 1. The mean difference between computed and measured line positions is small, only  $-0.4$  pixel. Eighteen out of 22 differences are negative, so a small systematic difference of order  $-0.1$  nm is not ruled out. The N I line at 921.053 nm has a large difference of  $-1.15$  nm. This line is free from sky lines and looks real but is a multiplet of lines at 918.997, 919.039, 919.210, 921.012, and 921.053 nm. The given value is for the last line in the blend, expected to be stronger. The measured position at 919.90 nm is at the center of the line, but the peak may be at 918.87 nm, suggesting that the earlier lines in the blend may be the strongest.

### Altitude, Speed, and Mass of the Meteoroid

The presence of weak metal atom ablation lines is not unusual for meteor spectra. The ratio of metal atom ablation lines versus air plasma emissions varies considerably from meteor to meteor and is particularly low for fast meteors ( $>30$  km/s) during normal ablation conditions in the absence of a high progressive fragmentation rate and flares from catastrophic breakup. Absent metal atom emissions may also point to a meteor captured relatively high in the atmosphere ( $>110$  km), where Mg-containing minerals do not yet ablate significantly (Borovička et al. 1999).

A shower identification would establish the velocity vector of the meteor. Unfortunately, the most obvious candidate is immediately dismissed. The meteor cannot be a particle of comet 1P/Halley, the parent of the eta-Aquarid shower (at 66 km/s), because the radiant of this shower was far below the horizon at the time of the event. The most active

among many minor showers that could be the source of this meteor is the ecliptic Southern May Ophiuchid ( $=\alpha$ -Scorpiid) shower with a radiant just east of Antares and with a 34 km/s entry velocity (Sekanina 1976), moving at an angle of  $\alpha \sim 64^\circ$  to the slit ( $90^\circ$  being perpendicular). The shower contributes only 1–2 meteors/hr to the meteor rate and is one of the stronger showers that night. However, lacking evidence for such a shower association, this meteor may have had any possible orientation between slit and meteor path (angle) and speeds between 11 and 72 km/s. The Southern May Ophiuchids are in the middle of this range.

If we use the Southern May Ophiuchid shower as an example, we find that the meteor would have been at an altitude of about 90 km (80–110 km) or a distance of about 104 km. The angular speed across the slit of the spectrograph would have been about  $13.7^\circ/\text{s}$ . The slit crossing time would have been only  $1/3600/13.7/\sin(64^\circ) = 2.3 \times 10^{-5}$  s. The light emission of a meteor peaks about  $1\text{--}2 \times 10^{-5}$  s after the meteoroid passes by and decays at any given position according to  $I(t) \sim t^{-1.4}$  (Jenniskens and Nielsen Forthcoming), for an effective exposure time of  $t_e = 7 \times 10^{-5}$  s (meaning that the integrated light intensity equals  $t_e$  times the peak intensity). Note that the long-lasting wake of forbidden O I green line emission does not fall in the spectral range observed here. Thus, the effective exposure time is a factor 3.0 times larger than the slit crossing time.

The flux of the spectrum has been normalized to continuum sources exposed during 1,200 s. If this crossing time is correct, then those flux values should be multiplied by  $1200/2.3 \times 10^{-5}/3$ , which would correspond to an absolute (at  $D = 100$  km) magnitude of  $-7.8$  magnitude ( $\sim 4.7 \times 10^{-13}$  W  $\text{cm}^{-2}$   $\text{\AA}^{-1}$ ) at 650 nm and the same as a mean over the range of 637–1050 nm. The meteor magnitude is usually defined as a mean over the full visual range of 400–700 nm that contains contributions from both ablation metal atom and air plasma emissions. In the unlikely complete absence of metal atom emissions, the visual magnitude might have been a magnitude fainter.

If the meteor moved at a shallow angle of only say  $20^\circ$  to the slit, then the meteor would have been a magnitude fainter. The meteor could have been a factor of two faster, which would change our estimate a factor of two brighter. In summary, we estimate that the meteor, while crossing the slit, had a mean brightness of  $-7.8 \pm 1.1$  magn. in the band (637–1050 nm).

### THE METEOR CROSS SECTION

To our knowledge, this spectrum permits the first direct measurement of the initial radius of a meteor and the distribution of light in the trail. The distribution of light along the slit is found to be nearly Gaussian, with a FWHM =  $14''$  (Fig. 4). This is ten times larger than the seeing ( $1.4''$ ) and resolves the volume of meteoric plasma in the direction along

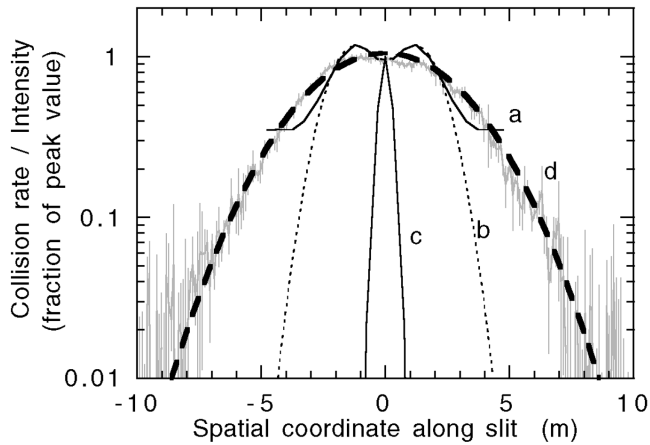


Fig. 4. The meteor trail cross section, expressed as the average intensity of N I and O I lines and the  $N_2$  molecular band along the slit. The result is compared to a Direct Monte Carlo Simulation calculation of the volume averaged collision rate of a 1-cm size Leonid at 95 km altitude (Boyd 2000), integrated along the meteor path and the line of sight, as a function of the third spatial coordinate along the slit. Curve (a) shows the collision rate of all molecules including those of the ambient air, curve (b) shows the result without ambient air molecules, while curve (c) shows the expected line profile if light emission occurs only for energetic collisions with  $N_2$  by including a term  $\exp(-E_a/kT)$ , with  $E_a = 7.2$  eV. Curve (d-dashed curve) is a scaled version of curve (c) to the observed line profile.

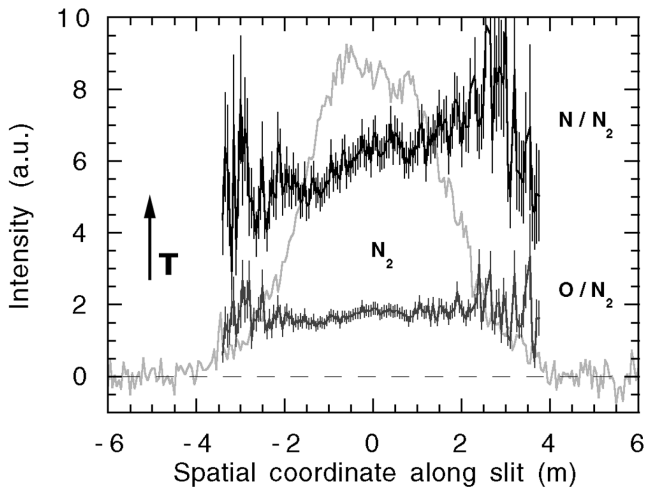


Fig. 5. Ratio of  $N/N_2$  and  $O/N_2$  intensities along the length of the slit from top (negative) to bottom (positive). The nitrogen band intensity profile is shown for comparison. The line ratios increase with temperature when a higher fraction of  $N_2$  is dissociated.

the slit. The  $FWHM = 7.0 (\pm 0.4) * \sin(\alpha) * (H \text{ (km)}/90)$  m, where  $\alpha$  is the unknown angle between the orientations of the slit and the meteor, and the numerical value applies for an assumed altitude of  $H = 90$  km. Note that there is a small but significant deviation from the Gaussian shape at the peak of the cross section profile (Fig. 4), which is seen in all strong lines and bands.

This width is thought to reflect the mean-free path in the ambient atmosphere and should not depend on meteoroid

mass or speed, as long as the meteoroid is in the rarefied flow regime, except for the speed dependence of the collision cross section:  $\sigma \sim V^{0.8}$  (Bronshten 1983). Earlier, measurements were obtained from photographic traces, finding dimensions of 1–6 m for altitudes around 90–100 km (Cook et al. 1959, 1962, and references therein). The accuracy of these measurements was usually poor because the trail width was significantly blurred by seeing and instrumental properties. However, our result is in agreement with Cook et al. (1962) if our meteor passed the slit at a reasonably tolerant  $\alpha = 8^\circ\text{--}58^\circ$ .

The mean-free path does depend on altitude. Hence, it is also possible that our meteor occurred at higher altitude than these photographed meteors, in which case the angle  $\alpha$  could have been closer to the ideal  $90^\circ$ . Experimental data from radar amplitudes of under-dense trails (assuming a Gaussian profile) show an increase of the initial trail diameter from 2.74 m at 92 km to 8.14 m at 112 km for speeds of 34 km/s (Baggaley 1970, 1980, 1981). This would suggest an altitude less than  $\sim 108$  km.

### Temperature Across the Meteor Trail

Although predictions for the meteor trail width are in general agreement with the observations, the shape of the profiles predicted by models is not. For starters, Jones (1995) presented results for a 2D simulation of the collision process for the gradually slowing down of impinging air molecules and their products during inelastic collisions with the ambient air. He found a strong deviation from a Gaussian profile, with a much higher core of electron densities at the center of the trail. Our observation of the distribution of emitted light does not show such an extended zone outside of the central core (Fig. 4).

Boyd (2000) developed a full 3D Direct Monte Carlo Simulation (DMSC) of the rarefied flow field around a 1 cm Leonid (71.6 km/s) meteoroid at 95 km altitude. Although Boyd predicts correctly a Gaussian decay of intensity, the model also predicts a Gaussian-shaped decrease of the kinetic temperature away from the meteoroid path. We will now show that this is not the case.

The kinetic temperature cannot be measured directly from the Doppler width of the lines because the instrumental apparatus function is larger than a typical Doppler-broadened line. However, there are several indirect measures that manifest themselves in the shape of the spectrum. Most importantly, a radial decrease of the kinetic energy will translate into a radial decrease of the ratio  $N/N_2$  and  $O/N_2$  in the plasma. This is mainly because an increase of plasma temperature leads to a rapid decrease in the mole fraction of  $N_2$  (Jenniskens et al. 2000, 2004a).

Figure 5 shows the variation of the ratios  $N/N_2$  and  $O/N_2$  along the slit. The remarkable result is that the  $N/N_2$  ratio varies by only 27% and the  $O/N_2$  ratio by only 11% across the trail. This variation indicates that the temperature gradient is small. The corresponding LTE plasma temperature that would produce such an  $N/N_2$  ratio is  $T = 4,340 \pm 20$  K at the trail

center and varies only from 4,300 to 4,365 K across the trail. At the trail edge, there is no significant change of temperature on the scale of the train width.

### Trail Width

With no variation in excitation temperature, the distribution of the light should match closely the distribution of collisions in the meteor wake, integrated along the meteor path. About 3% of the thermal collisions are thought to be inelastic (Öpik 1958), leading to optical emissions. The volume-averaged collision rates calculated by Boyd (2000) were averaged along the meteor path and the line of sight, and are shown in Fig. 4 as a function of the third spatial coordinate along the slit. The result is compared to the meteor trail cross section as derived from the average intensity of N I and O I lines and the N<sub>2</sub> molecular bands along the slit. Curve (a) shows the collision rate of all molecules including those of the ambient air, while curve (b) shows the result without ambient air molecules. Curve (b) is broader than a single Gaussian profile and is well-matched by a sum of two Gaussian profiles ( $\sim \exp[-([z(m) - z_0]/2)^2]$ ), displaced from the center by  $z_0 = 1.3$  m and with a dispersion  $\sigma = 1.4$  m. Such a shape might be expected if the meteoroid consists of two large fragments.

However, only collisions energetic enough will lead to optical emissions. Curve (c) shows the expected line profile if light emission occurs only for energetic collisions of N<sub>2</sub> and metal atoms with the ambient atmosphere, calculated by including a term  $\exp(-E_a/kT)$ , with  $E_a = 7.2$  eV, where  $T$  is the calculated gas temperature profile. It is clear from this figure that the width of the trail as seen in emitted light is limited by the  $\exp(-E_a/kT)$  term and is significantly narrower than the distribution of all collisions.

We conclude that the observed trail is much wider than expected from current meteor expansion models when taking into account the observed gas temperature profile. Curve (d) is a scaled version of curve (c) to the observed line profile if the emission would derive from a higher altitude and/or the meteor crossed the slit at a smaller angle  $\alpha$ . If this broadening is due to emission being from higher altitude (assuming  $\alpha = 90^\circ$ ), then this would demand an unreasonable altitude ( $>200$  km). If the broadening is due to a smaller angle  $\alpha$ , then for a reasonable altitude of 90 km, this demands a small angle  $\alpha = 3^\circ$ , with the meteor moving nearly along the meteor slit. Although this is not impossible, the probability for such fortuitously aligned trajectory is small. More importantly, such small angle alone does not explain the observed temperature profile. Other processes may explain both the relatively large width and temperature profile.

### Sources of Trail Broadening

The temporal variation of light emission from a model meteor was studied by Jenniskens and Nielsen (2004) from

observed high frame-rate images of meteors and the model by Boyd (2000). It was found that half of the light is recorded in the first  $1.1 \times 10^{-4}$  s and 90 percent after 6 ms, with an effective exposure time of only about  $7 \times 10^{-5}$  s. After 6 ms, the stars have only moved an angle of  $0.09''$ . Therefore, the train width cannot be influenced by the tracking of the telescope on the stars instead of the train.

After formation, the cooling air plasma drifts according to the prevailing winds, which can be up to  $\sim 100$  m/s perpendicular to the line of sight. The meteor follows a straight line, but after deposition, the decaying light drifts about 6 pixels (0.6 meter) in 6 ms. That is much less than the observed trail width. Moreover, any such drift should have resulted in an asymmetry in the trail profile, which is not observed. Therefore, the train width is not broadened significantly by the drift of the train due to upper atmosphere winds.

### Defocussing

Sadly, the most likely explanation for the wide trail is that the meteor, even at 100 km altitude, is out of focus. The defocus  $d$  can be written as:

$$d = \cos(\varphi) * (Df)^2 / H \quad (1)$$

where  $\varphi$  is the zenith angle ( $29.8^\circ$ ) and  $H$  the altitude of the object, while  $D$  is the diameter of the telescope ( $=8$  m), and the  $f$ -number is that of the Cassegrain focal plane ( $f = 13.4$ ), which is re-imaged by the FORS spectrograph. This gives a defocus FWHM of 128 mm. With an imaging scale of 0.1 arcsec for 1 mm, this would give a width of  $12.8''$  at  $H = 90$  km. This approximate result was checked using a ray tracing program, which gave values of  $16''$  for  $H = 90$  km,  $14''$  for 100 km, and  $12''$  for 150 km. Our measured width of  $14''$  suggests that the meteor was captured at 100 km altitude, which is in good agreement with the expected location of peak brightness.

Unlike our expectations, the trail was not resolved, and the measured width was only an upper limit. This explains the near constant excitation conditions throughout the emitting volume and the fact that the volume is larger than expected.

### SEARCH FOR CARBON ATOM EMISSION

There is no evidence that this meteor spectrum contained emission from metal atoms derived from the minerals in the meteoroid. That does not exclude the possibility of emission from the more volatile organic matter contained in the meteoroid.

Organic matter is expected to be present in meteoroids, but it is still not known whether that organic matter is fully atomized in the meteor ablation process. Earlier searches of breakup products, such as CN, have not been successful

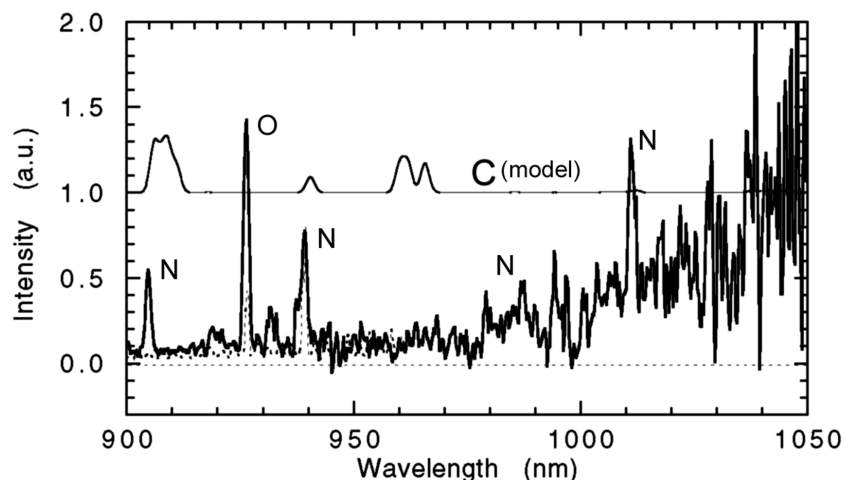


Fig. 6. The newly opened wavelength range from 900 to 1050 nm, with the superimposed air plasma model (dashed line). A similar model for LTE C I line emission at 4,340 K is displaced upward by 1 unit to facilitate comparison. The rise of the spectrum toward long wavelengths is possibly an artifact of the reduction process because the signal is weak and the instrument response is falling off.

(Rairden et al. 2000; Jenniskens et al. 2004b). If a significant fraction is atomized, this could result in emission from neutral carbon atom (C I) lines that can be detected in the relatively unexplored spectral range above 900 nm. More importantly, carbon atom emission is also expected from atmospheric CO<sub>2</sub>, which breaks into its atomic constituents in LTE conditions at T ~4,400 K (Jenniskens et al. 2000).

All carbon atom lines at visible wavelengths have low Einstein A coefficients and are weak. The most intense lines are expected in the near-IR (given in Table I for reference) and the far UV wavelengths. Recently, Carbary et al. (2003) have reported the tentative detection of neutral carbon atom lines in the emission of a Leonid fireball (afterglow) at far-UV wavelengths. The ESO/VLT spectrum offers a window on the 900–1050 nm region of the spectrum (Fig. 6), which, until now, remained relatively unexplored.

We readily identify strong candidate lines at 905 and 939 nm, but these are 1.0 and 1.8 nm off from the anticipated emissions from C I. This discrepancy is much larger than our wavelength calibration errors. Instead, these lines are identified with atomic emissions from nitrogen. The 905 nm line identification remains somewhat uncertain because the LTE model predicts a much weaker line.

An upper limit to the total carbon atom abundance in the air plasma is calculated following Jenniskens et al. (2004b). Especially, the region from 906 to 910 nm offers little interference from the sky airglow background. From a comparison of noise at those wavelengths with the intensity of the oxygen 926 nm lines, we find for the ratio of neutral components:  $[C]/[O] < 2 \times 10^{-4}$ . Most oxygen is in atomic form. Most carbon atoms are also expected to be in neutral form. The ionization potential for carbon is as high as that for oxygen and nitrogen, and charge transfer occurs easily with metal atom ablation products. Hence, the anticipated fraction of C<sup>+</sup> is small. We calculated that an LTE air plasma at 4,400

K with the pressure and composition of air at 95 km altitude would have an expected abundance of  $[C]/[O] = 7 \times 10^{-4}$ .

Although this value is no more than three sigma higher than our measured upper bound, we conclude that not all atmospheric CO<sub>2</sub> is dissociated into CO + O and then atomized, as would be expected in LTE conditions and during impacts. This implies that meteors are not as efficient as might be expected in aerothermochemistry of an early Earth atmosphere. Without quantitative analysis of the carbon abundance derived from the far-UV data, we cannot decide whether this argues against the identification of neutral carbon lines by Carbary et al. (2003).

Unfortunately, no metal atom line emission is detected in the spectrum that could help relate the upper limit of carbon emission to meteoric ablation products. The expected number density of meteoric vapor in the meteor plasma is about  $1.0 \times 10^{-2}$  per O atom (Boyd 2000). If so, less than one in a hundred meteoric vapor atoms are carbon. If the ratio of organic refractory mass versus silicate mass is 0.88 (Greenberg 2000), then the carbon atom abundance should have been about  $[C]/[O] = 4 \times 10^{-3}$ , suggesting that perhaps less than 1 in 20 carbon atoms is vaporized in atomic state. Other meteoric carbon may survive the ablation process in the form of small or complex reduced organic molecules or in solid grains, providing potential prebiotic molecules at the time of the origin of life (Jenniskens et al. 2000).

## CONCLUSIONS

We conclude that the anomalous signal detected at the ESO/VLT was in fact a meteor of brightness  $-7.8 \pm 1.1$  magnitude. The variation of spectral features across the slit shows that the ratio of atomic and molecular nitrogen emission is surprisingly constant in the whole volume of the emitting plasma. We conclude that this is mainly due to the

fact that the trail is out of focus, a problem that will persist in future observations of meteor trails with large telescopes focussed at infinity.

From the lack of carbon atom emission in the spectrum, we conclude that the air plasma did not efficiently dissociate atmospheric CO<sub>2</sub> into atomic carbon at the level expected for LTE conditions, but our measured upper limit abundance of neutral carbon atoms is only 3 sigma below that expected.

*Acknowledgments*—The raw data of this serendipitous observation were kindly made available for analysis by Dr. C. Lidman (ESO) on behalf of the SCP collaboration. Derrick Salmon of CFHT first pointed the possible defocus problem out to us. Henri Bonnet and Markus Kasper from the ESO artificial laser guide star (LGS) program helped compute the defocus at the Cassegrain focus. Jason Spyromilio performed the ray tracing calculations. This work is supported in part by NASA's Astrobiology and Planetary Atmospheres Programs.

*Editorial Handling*—Dr. Carlé Pieters

## REFERENCES

- Baggaley W. J. 1970. The determination of the initial radii of meteor trains. *Monthly Notices of the Royal Astronomical Society* 147: 231–243.
- Baggaley W. J. 1980. Measurements of the velocity dependence of the initial radii of meteor trains. *Bulletin of the Astronomical Institute of Czechoslovakia* 31:308–311.
- Baggaley W. J. 1981. Single wavelength measurements of the initial radii of radio meteor ionization columns. *Bulletin of the Astronomical Institute of Czechoslovakia* 32:345–349.
- Borovička J. 1993. A fireball spectrum analysis. *Astronomy and Astrophysics* 279:627–645
- Borovička J., Stork R., and Bocek J. 1999. First results from video spectroscopy of 1998 Leonid meteors. *Meteoritics & Planetary Science* 34:987–994.
- Borovička J. and Zamorano J. 1995. The spectrum of fireball light taken with a 2-m telescope. *Earth, Moon, and Planets* 68:217–222.
- Boyd I. D. 2000. Computation of atmospheric entry flow about a Leonid meteoroid. *Earth, Moon, and Planets* 82–83:93–108.
- Bronshten V. A. 1983. Luminosities and spectra of meteors. In *Physics of meteor phenomena*. Dordrecht: D. Reidel. 165 p.
- Carbary J. F., Morrison D., Romick G. J., Yee J.-H. 2003. Leonid meteor spectrum from 110 nm to 860 nm. *Icarus* 161:223–234.
- Ceplecha Z. 1973. A model of spectral radiation of bright fireballs. *Bulletin of the Astronomical Institute of Czechoslovakia* 24:232–242.
- Cook A. F. II, Hawkins G. S., and Steinson F. M. 1959. The width of meteor trails II. *The Astronomical Journal* 64:327–327.
- Cook A. F., Hawkins G. S., and Steinson F. M. 1962. Meteor trail widths. *The Astronomical Journal* 67:158–162.
- Greenberg J. M. 2000. From comets to meteors. *Earth, Moon, and Planets* 82–83:313–324.
- Harvey G. A. 1973. Elemental abundance determinations for meteors by spectroscopy. *Journal of Geophysical Research* 78:3913–3926.
- Jenniskens P. and Stenbaek-Nielsen H. 2004. Meteor wake in high frame-rate images and implications for the thermal processing of ablated organic compounds in air. *Astrobiology* 4:95–108.
- Jenniskens P., Laux C. O., Packan D. M., Wilson M., and Fonda M. 2000. Meteors as a vector for the delivery of organic matter to the early Earth. *Earth, Moon, and Planets* 82–83:57–70.
- Jenniskens P., Laux C. O., Wilson M., and Schaller E. 2004a. The mass and speed dependence of meteor plasma temperatures. *Astrobiology* 4:81–94.
- Jenniskens P., Schaller E. L., Laux C. O., Schmidt G., and Rairden R. L. 2004b. Meteors do not break exogenous organic molecules into di-atoms. *Astrobiology* 4:67–79.
- Jones W. 1995. Theory of the initial radius of meteor trains. *Monthly Notices of the Royal Astronomical Society* 275:812–818.
- McKinley D. W. R. 1961. *Meteor science and engineering*. New York: McGraw-Hill. 309 p.
- Millman P. M. 1949. One hundred meteor spectra. *The Astronomical Journal* 54:177–178
- Millman P. M. 1980. One hundred and fifteen years of meteor spectroscopy. In *Solid particles in the solar system*, edited by Halliday I. and McIntosh B. A. Dordrecht: D. Reidel. pp. 121–128.
- Öpik E. J. 1958. *Physics of meteor flight in the atmosphere*. New York: Interscience Publishing. 174 p.
- Rairden R. L., Jenniskens P., and Laux C. O. 2000. Search for organic matter in Leonid meteoroids. *Earth, Moon, and Planets* 82–83: 71–80.
- Sekanina Z. 1976. Statistical model of meteor streams. IV—A study of radio streams from the synoptic year. *Icarus* 27:265–321.